

Article

Environmental Decay of Ignimbrite Patrimonial Monuments in the Dry, Urban, and Non-Industrial Atmosphere of Morelia (México)

Rosalia Ruiz-Ruiz ^{1,2,*}, Elia Mercedes Alonso-Guzman ^{1,*}, Wilfrido Martinez-Molina ¹,
Hugo Luis Chavez-Garcia ¹, Mauricio Arreola-Sanchez ^{1,3}, Jorge Alberto Borrego-Perez ^{1,3},
Marco Antonio Navarrete-Seras ¹, Judith Alejandra Velazquez-Perez ^{1,2} and Luis Alberto Morales-Rosales ³

¹ Faculty of Civil Engineering, Universidad Michoacana de San Nicolás de Hidalgo, Morelia 58070, Mexico
² Doctoral Program in Civil Engineering, Faculty of Civil Engineering, Universidad Michoacana de San Nicolás de Hidalgo, Morelia 58070, Mexico
³ CONACYT, Universidad Michoacana de San Nicolás de Hidalgo, Morelia 58070, Mexico
* Correspondence: rosalia.ruiz@umich.mx (R.R.-R.); elia.alonso@umich.mx (E.M.A.-G.)

Abstract: Damage to the rocks of historic built heritage needs to be addressed to facilitate their conservation and restoration; the most serious damage is caused by environmental conditions and human activities. Buildings constructed with ignimbrite blocks bonded with lime mortar in Morelia, México, a UNESCO World Heritage site, were studied. The damage mainly occurs in the facades, on the surfaces of the rocks and in the mortar of the union exposed to climatic factors such as sun, rain, wind, and temperature changes, due to the actions of humans and vehicles emitting polluting gases; and due to pigeon excrement. This has caused the formation of patinas and flora, reduced the mechanical strength and exfoliation, decreased the density and cohesion in the mortar with rocks, and led to friction damage caused by people. In the facades of five buildings, the mechanical resistance and microstructural characteristics were indirectly determined by XRD, XRF, and SEM. The results were related to the climate, humans, and vehicular pollutant emissions. The damage was due to the environment, the influencing geographic orientation, and prevailing winds, rising capillary water on the facades, pigeon droppings, vehicular pollutant gases, and humans. Potential banks of healthy quarries were analyzed for use in the conservation and restoration of damaged monuments.

Keywords: historical heritage; environmental; stones; sclerometer; physical-mechanical properties; ignimbrite blocks



Citation: Ruiz-Ruiz, R.; Alonso-Guzman, E.M.; Martinez-Molina, W.; Chavez-Garcia, H.L.; Arreola-Sanchez, M.; Borrego-Perez, J.A.; Navarrete-Seras, M.A.; Velazquez-Perez, J.A.; Morales-Rosales, L.A. Environmental Decay of Ignimbrite Patrimonial Monuments in the Dry, Urban, and Non-Industrial Atmosphere of Morelia (México). *Heritage* **2023**, *6*, 3137–3158. <https://doi.org/10.3390/heritage6030167>

Academic Editors: Andrea Macchia, Fernanda Prestileo and Alexandra Jeberien

Received: 1 February 2023
Revised: 10 March 2023
Accepted: 13 March 2023
Published: 15 March 2023



Copyright: © 2023 by the authors. Licensee MDPI, Basel, Switzerland. This article is an open access article distributed under the terms and conditions of the Creative Commons Attribution (CC BY) license (<https://creativecommons.org/licenses/by/4.0/>).

1. Introduction

At present, the user preferences for natural stones in the construction sector, especially as floor covering elements for interior and exterior use in buildings, show an increasing trend day by day [1]. Pyroclastic rocks have been widely used in the construction of historical monuments, but they are very susceptible to the deterioration process, which can be understood as the process in which rocks are transformed due to agents present in the built environment, such as salt, water, ice, biological colonization, atmospheric pollution, etc. [2,3]. The following is a brief review of the main types of deterioration of heritage buildings.

1.1. General Decay Due to Natural Weathering

Cultural heritage is widely recognized to be at risk due to the impact of climate change and associated risks such as torrential rainfall, floods, and droughts. User-driven solutions are urgently needed for the sustainable development and protection of monumental ensembles and related collections that are exposed to changes in extreme climate [4].

Weathering of geomaterials can be amplified by meteorological conditions such as wind action, which is one of the main causes of degradation affecting the surfaces of

monuments. The effect depends on the strength, direction, and speed of the wind, the impact of the transported particles and their size, as well as the characteristics of the affected surface [5,6].

Various works have been carried out on the effect of wind on the deterioration of built heritage, from experimental work [7] and microscopy and numerical simulations [8–10] to proposals for coatings to reduce deterioration [6] and the design of devices that allow for monitoring of physical and chemical changes due to weathering [11]. Michette et al. [12] hypothesized that powdering and flaking decay patterns are a direct consequence of climatic factors but found that the determining factor is the physical variation of the stone.

Damage due to wind ranges from loosening of loose material to pitting and gullying in the case of wind-driven rain, which has a great impact on moisture conditions, as it modifies the response to rainwater impact, maximizing erosion and causing anisotropic deterioration in buildings [7,13]. Wang et al. [10] found that at velocities of 10 m/s, corners facing the prevailing winds, doors and windows on open sides, locations where swirling winds develop, and eaves of sloping roofs of buildings suffered more severe erosion.

Moisture properties, i.e., capillary sorption, water sorptivity, and salt crystallization may also be related to deterioration processes [14]. The presence of water in building stones is another major factor in the deterioration of masonry monuments due to natural weathering. When natural stones used as building cladding elements meet a water source, the water moves along the cracks and/or matrix structures by capillarity and penetrates the rock. Over time, this phenomenon degrades the physical and mechanical properties of the structures due to the atmospheric conditions and chemical properties of the material, including the freezing temperature of the water that is contained in the pores and expands. This temperature is locally present at dawn [1].

Capillary rise is the most common mechanism of water penetration into building materials and the most effective parameter in the evaluation of this process [2,14–17]. The capillary absorption coefficient can vary depending on many parameters, such as the degree of anisotropy and the orientation of the rocks, as well as the density, geometry, size, and structure (closed or connected to each other) of the pores [1,14]. The amount of water penetrating the rocks and the rate of this penetration play a crucial role in accelerating the rock deterioration process [16].

Crystallization of salt and ice in pore spaces causes significant physical damage to natural building stones, which can be attributed to the physical stress induced in the rock during crystallization. Crystallization weathering, in freeze–thaw cycles, depends on the characteristics of the stones and their porosity, water transport, and mechanical properties [18]. Soluble salts are compounds found inside ornamental rocks and building stones exposed to atmospheric agents in environments rich in alkaline metal ions, such as sodium and potassium. Sodium sulfate is one of the most common and harmful salts found in constructions under these conditions [19].

1.2. General Decay Due to Anthropogenic Source

Atmospheric pollutants act as catalyzers for the deterioration processes of the materials of civil works, which generates large economic losses due to repair and maintenance works, but when it comes to buildings that are also of great historical and cultural importance, they cause premature aging and reduce their aesthetic value [20–24]. The use of aerosols, oil, and gas generates carbonaceous fractions that are the main contributor to atmospheric pollution [25]. The most aggressive pollutants that lead to the deterioration of the rocks of heritage monuments are CO₂, SO₂, nitrogen oxides (NO_x), ozone, and atmospheric particles, generated mainly by anthropogenic sources such as vehicle traffic and industrial activities in urban areas [26–29].

Different pollutants affect and generate different types of damage; for example, sulfur oxides (SO_x) [30] on calcareous stones can transform into CaSO₄ with consequent solubilization and the formation of black crusts [31]. The deposition of atmospheric particles resulting from urban pollution on heritage buildings causes an aesthetic impact, a black

crust, but when these particles meet water, chemical reactions occur that intensify the surface damage [32]. Barca et al. [26] found that the deposition of heavy metals on black crust depends on the shape and exposure of the surface. Another type of pollutant affecting buildings is dirt deposited on facades exposed to atmospheric particles such as a particulate matter of 2.5 and 10 microns ($PM_{2.5}$ and PM_{10}), which has increased in recent years [33]. Particulate matter contains acidic species and carbonaceous particles that can act as a catalyst forming nitric and sulfuric acids [34]. Dew combined with high carbon dioxide (CO_2) and sulfur dioxide (SO_2) concentrations in the air of built-up urban environments can deposit weak acids on a building's surface. Both affect stone by causing chemical erosion, where the dissolution of $CaCO_3$ occurs and causes the surface of the stone to gradually erode and wash away [35].

The effects of climate change on historical and cultural heritage buildings will increase as human activities and needs continue to generate greenhouse emissions and changes in atmospheric conditions. Studies could help prevent and conserve heritage buildings without compromising human comfort [36,37].

1.3. Biological Decay

The main damage to monuments by biodeterioration is caused by microorganisms such as fungi, algae, bacteria, actinomycetes, and protozoa, but also by rodents, birds, plants, and humans [38–40]. Biological colonization can contribute directly and indirectly to the deterioration of stone, either by using it as a substrate or by imposing physical stress, serving as nutrients for other organisms or providing compounds (calcium oxalates and carbonates) for secondary chemical reactions [41,42]. The mechanisms of biodeterioration are very diverse; the best known are biofilm formation, discoloration, salting, physical damage, inorganic and organic acids, and osmolytes.

The most common biofilms are green and black–gray biofilms which are the result of massive colonization by algae and fungi, respectively [39,40]. Scheerer et al., Vlasov et al., and Zhang et al. [38,41,42] analyzed the composition of microbial communities, their effects, and their relationship with environmental factors. Zhang et al. [42] found that several culturable fungal strains were able to produce pigments, and others showed potential for biomineralization by precipitation of calcite and weddellite. Gaylarde [41] mentions that cyanobacteria are probably the most important colonizers of stone buildings, as they are not dependent on any organic carbon source and are very resistant to environmental changes. López-Moreno et al. [43] isolated heterotrophic $CaCO_3$ -precipitating bacteria from biofilms on deteriorated ignimbrites from Morelia (México). In the study, they identified three types of bacteria: *Enterobacter cancerogenus*, *Bacillus* sp., and *Bacillus subtilis*. They found that in a solid medium, the first two precipitated calcite and vaterite, while *Bacillus subtilis* only precipitated calcite.

Colonization by plants occurs due to the combination of biotic and abiotic factors, such as sunlight, orientation, local climatology, the microclimate of the monument, and the presence of water, and air pollution, among others, which create the necessary conditions for the formation of suitable substrates for the development of lichens, mosses, and vascular plants, mainly [44,45]. Lichens cause chemical and mechanical damage to heritage rocks; the former decompose lithics through the production of citric, oxalic, lactic, and gluconic acids; the mechanical ones cause loss of cohesion due to hyphal penetration [46,47]. Mosses retain water and nutrients that favor the growth of microorganisms that can form a protective layer. However, excess moisture promotes rock deterioration and weathering [48–50]. Vascular plants are considered the most harmful causes of deterioration due to the radial growth of their roots; higher pressures are generated in the structural materials causing cracking and a lack of adherence, which generates stability and safety problems [46,51].

Another form of damage to masonry monuments due to biological deterioration is caused by pigeon feces, which causes damage to surfaces in the first two weeks following their deposition, but then they are dissolved [52–55]. The effects derived from this are: the introduction of viable seeds of vascular plants; the visual deterioration of the surfaces by

stains; the chemical deterioration of the surfaces by the introduction of acids (phosphoric, nitric, and uric) and soluble salts; and the deposition of nutrients that help biodeterioration by bacteria, fungi, and lichens. Alternatives have been sought to protect monuments from the damage caused by pigeons; the most common protection method is the application of protective layers of oleo/hydrophobic polymers to exposed surfaces [56].

There exists different research focused on finding techniques to preserve stones and avoid their progressive deterioration. They are mainly based on finding coatings or replacing the stone material with materials with very similar characteristics. An example is the application of 2 g/m² of a nanocomposite in powder/binder proportions equal to 1% *w/v* of TiO₂, which provides a suitable hydrophobic character to the stone material with acceptable chromatic variations [57]. Another example is barium hydroxide which is used as a rock-reinforcing agent that partially fills the porosity with an inorganic by-product in the form of acicular crystals based on pure barium carbonate, thus avoiding the total closure of the pores and respecting the permeability of the material [58]. There are different techniques for the study of heritage stones, and the most widely used is the application of non-destructive testing (NDT) which can detect problems imperceptible to the naked eye, thus avoiding possible losses [59,60]. One of the methods used is infrared thermography, which allows for the recognition and mapping of different surface temperatures derived from the presence of efflorescence, sub-efflorescence, alveolarization, black crusts, and bio-aging in limestone and basaltic rocks, thus making it a rapid diagnostic tool for weathering [61–63].

This research focuses on the study of the deterioration of historic buildings in the city of Morelia, which was founded in 1541 and is the Mexican city with the most buildings classified as historic monuments. It has 1130 civil and religious historical monuments, of which 260 were identified as relevant. The city was included in UNESCO's World Cultural Heritage List on 12 December 1991 [64] since the urban perspectives of the historic center of Morelia constitute "a unique model in America", which is made up of works built from the seventeenth century to the post-modern twentieth century [65]. Morelia has an original architectural style that combines previous and more recent styles (medieval, renaissance, and neoclassical) [66]. The buildings are made of masonry with pink ignimbrite rocks, which has led it to be known as "the pink stone city" [67].

2. Materials and Methods

2.1. Monuments under Study

The monuments under study are shown in Figure 1, and they were: Morelia Metropolitan Cathedral (CAT), the Primitive and National College of San Nicolas (SAN), Capuchinas church (CAP) of the order of Franciscan or Capuchin nuns, the Regional Museum of Michoacan (MR), and the Carmen church (CC); the buildings that are in the historic center of the city are described below.

Morelia is in the north-central region of México and is settled over a hill of Guayangareo Valley, a quarry of rhyolitic ignimbrite which was used to build all of the historic buildings in the center of the old Valladolid city (the name used before the current Morelia name) [68,69]. The geology of the Morelia region is composed of lacustrine sediments derived from Cuitzeo Lake and volcanic materials from the Quinceo–Tetillas volcanoes and Indaparapeo, Garnica, and Punhuato volcanic complexes [70]. The characteristics of the ignimbrites used in the historic buildings in Morelia correspond to the different materials that comprise pink welded ignimbrite, such as pumices and lithics in a well-consolidated matrix.

The Metropolitan Cathedral of Morelia (CAT) was built from 1660 to 1744. It is an enormous colossus of pink stone with two large towers of 66.8 m in height, the second tallest in México, with a baroque style. It has a triple facade (one front and two sides) with carved altarpieces. The temple has a Latin cross plan with a length of 96 m and a total width of 62 m. Bordering the atrium is a beautiful wrought iron grille dating from the nineteenth century [71].

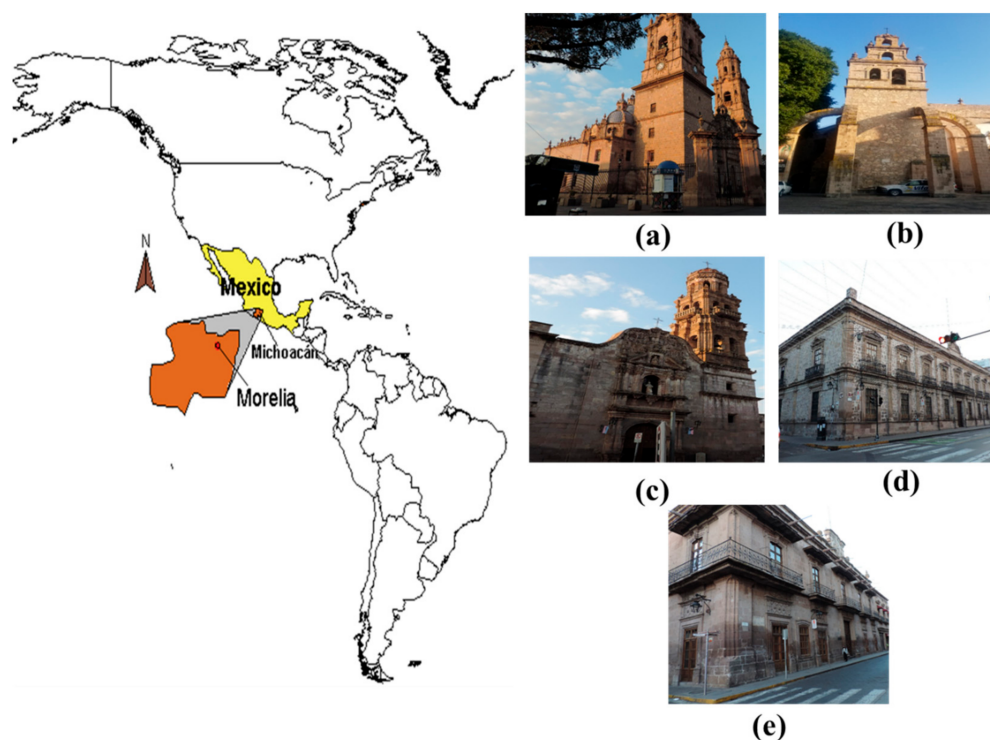


Figure 1. (a–e) Historic center: geographical location (America, México, Michoacán, Morelia) and main buildings: (a) the cathedral (CAT), (b) Carmen church (CC), (c) Capuchinas church (CAP), (d) San Nicolás College (SAN), and (e) Michoacán Museum (MR).

The Primitive and National College of San Nicolás (SAN), built in the seventeenth century during the viceregal period, has functioned since then as an educational institution where the national heroes Hidalgo, Morelos, and Ocampo studied. The building has undergone reconstruction several times during its life, although the facade managed to conserve a certain sober baroque style, which harmonizes with the rest of the surrounding buildings [72].

Capuchinas church (CAP), built in the third decade of the seventeenth century, is outside the walls of a small chapel where the image of a virgin was venerated. The convent belonged to the Clarissa nuns of the San Francisco rule. The baroque style of its facade, with fine Corinthian columns, is evidence of a strong popular accent [73].

The Regional Museum of Michoacán (MR) was built between 1705 and 1775; it is a typical palatial construction of Morelia baroque style that stands out due to its quarry facade, the fine carving of the door and balconies, as well as the arches of the courtyard. It is also one of the oldest museums in the country [74].

Carmen church (CC) was built on a Latin cross plan and is distinguished by its four domes built in the seventeenth century. The main facade facing west has the coat of arms of the order, and the cloister has a single floor of small dimensions and is surrounded by four portals [75]. This building was built for the nuns of the Carmelite order.

All of the architectural heritage mentioned above belong to the historic monument zone, with a civil and religious architecture built between the seventeenth and nineteenth century upholding the original layout of the sixteenth century's old Valladolid town. The historic buildings were built using ignimbrites as the main construction material; the use of pink stone contributes to the homogeneity perspective of the historic downtown area.

For the present publication, the above historical monuments were chosen because of their mechanical compressive strength data, estimated by means of non-destructive sclerometric tests with a Schmidt hammer, as well as information on the microstructure of the rocks, determined with the following techniques: scanning electron microscopy (SEM), X-ray diffraction (XRD), and X-ray fluorescence (XRF). The following is a summary of the

studies carried out on the buildings studied. With the examples of historical heritage, to carry out research, it is necessary to obtain permission from the corresponding federal authorities, which in this case is the National Institute of Anthropology and History (INAH). Therefore, the information obtained is the product of a lot of management and was obtained partially, as shown in Table 1.

Table 1. Methods to determine the properties of ignimbrites.

	Test	Ignimbrite Quarry or Historical Monument
Identification and classification properties	X-Ray diffraction (XRD)	* Cointzio and Jamaica. ** CAT, CAP, and SAN
	Scanning electron microscopy (SEM)	** CAT and SAN
	X-ray fluorescence (XRF)	* Cointzio, Jamaica, and Tejocote. ** CAT, CAP, and SAN
	Apparent density, % water absorption, specific gravity	* Cointzio, Jamaica, and Tejocote. ** CAT, CAP, SAN, and CC
Mechanical properties	Uniaxial compressive strength (UCS) of stone cubes	* Cointzio, Jamaica, and Tejocote. ** CAT, CAP, SAN, and CC
	Estimation of UCS with a Schmidt hammer	** CAT, CAP, SAN, CC, and MR

* Cointzio (Coin), Jamaica (Jam), and Tejocote (Tej). Ignimbrite quarry potential for the restoration of historical monuments. ** CAT, CAP, SAN, CC, and MR. Monuments under study.

2.2. Environmental and Climatic Conditions in Morelia

The above monuments are exposed to the environmental contamination and climatic conditions of the city of Morelia, in which a sub-humid temperate climate predominates, its annual average temperature is 17.5 °C, and the precipitation is 773.5 mm per year. The prevailing winds come from the southwest (SW) and northwest (NW), which are variable in July and August, with speeds of 2.0 to 14.5 km/h [76]. According to the National Air Quality Report 2020, the main pollutants in Morelia were suspended particles of 2.5 and 10 microns, with the highest concentration from March to May; O₃, with the highest concentration from March to June; CO, NO₂, and SO₂. The concentrations are measured in accordance with the standard limits for health protection. The annual concentration of PM_{2.5} was 16 g/m³, that of ozone was 0.081 ppm for 8 h, and that of NO₂ was 0.04 ppm per hour. The concentrations of the other pollutants are not reported due to insufficient information [77].

The generation of the main atmospheric pollutants in Morelia is shown in Figure 2. The figure includes the total annual emissions, both fixed and mobile. Figure 2b shows a notable reduction in environmental pollutants in recent years due to the fact that the Mexican Official Standard NOM-041-SEMARNAT-2015 [78], which establishes the maximum permissible limits for the emission of polluting gasses from the exhaust of motor vehicles in circulation that uses gasoline as fuel, came into force in 2007. However, pollution from these gasses continues to be considerable and is an important factor in the deterioration of materials.

Different climatic changes together with the pollution produced by vehicular traffic and public transportation, have caused a gradual deterioration in historical heritage. Figure 3 shows the average maximum annual precipitation in millimeters and the average maximum annual temperature from 1990 to 2002, which has generated wet–dry cycles over the years on the facades. A sharp decrease in average precipitation has been observed from 2020 to date, as well as a drastic decrease in maximum precipitation in 2020. On the other hand, Figure 4 shows important changes in solar radiation and atmospheric pressure, which have increased and decreased since 2014, respectively. Therefore, there is a change in climatic conditions that are reflected in the deterioration of historical monuments.

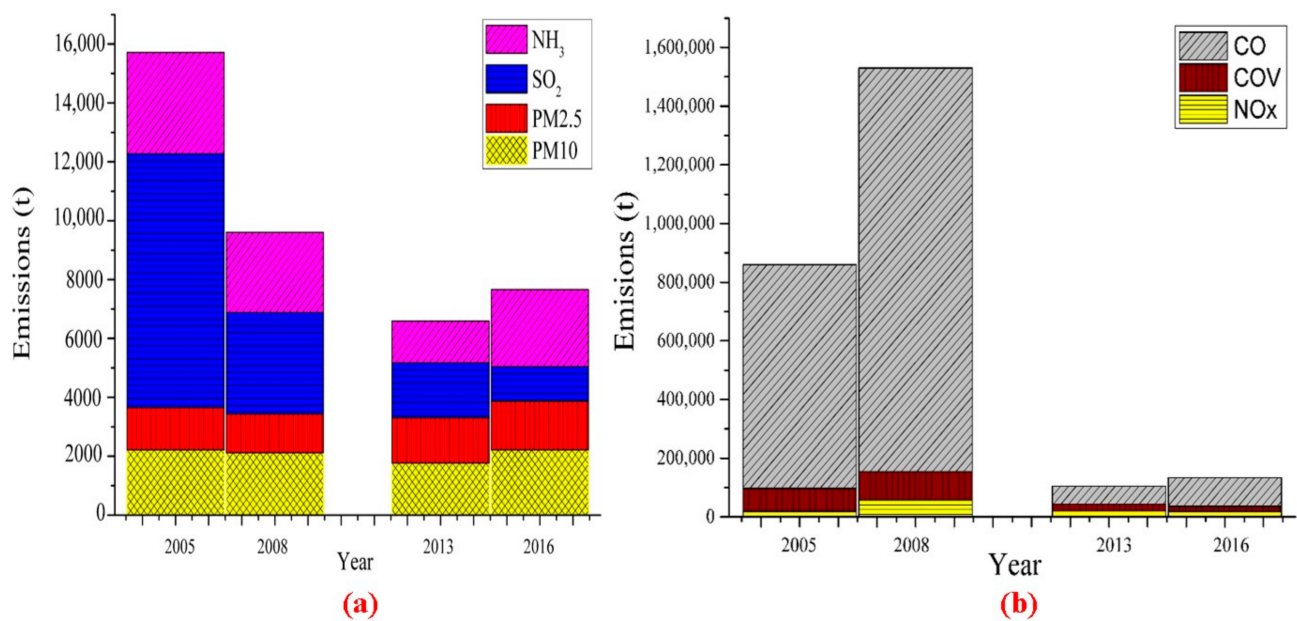


Figure 2. Atmospheric pollutants in Morelia, Michoacan, México: (a) NH₃, SO₂, PM_{2.5}, and PM₁₀; (b) CO, COV (volatile organic compounds), and NO_x. Source: National Pollutant Emission Inventories [79].

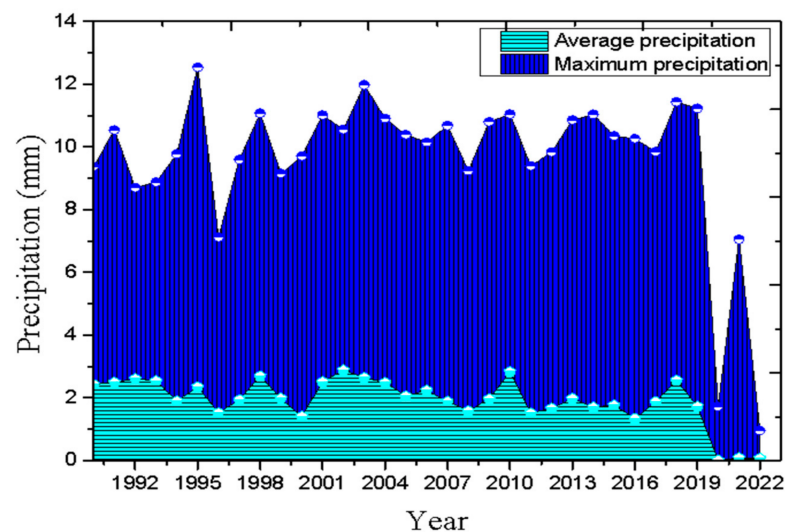


Figure 3. Minimum and maximum precipitation in Morelia, Michoacan, México.

On the other hand, an increase in the minimum and maximum temperature (Figure 5) has been observed, especially in recent years. The minimum temperatures close to 0 °C cause freezing of the water inside the pores which, when it expands, causes microcracks and exfoliation. Figure 6 shows the maximum annual wind speed and relative humidity, which have increased and decreased in the last five years, respectively. The average velocity indicated in the table cannot be considered as a precursor of mechanical decay, but it does transport PM 5, which is mostly deposited on the facades facing the prevailing winds. The dominant direction in Morelia is S and S-SW, and in that direction, there is a paper and glue factory, whose pollution is transported to the center of the city. The same figure shows that it has a dry and urban atmosphere with almost one million residents. The sum of these factors is accelerating the deterioration of historic buildings.

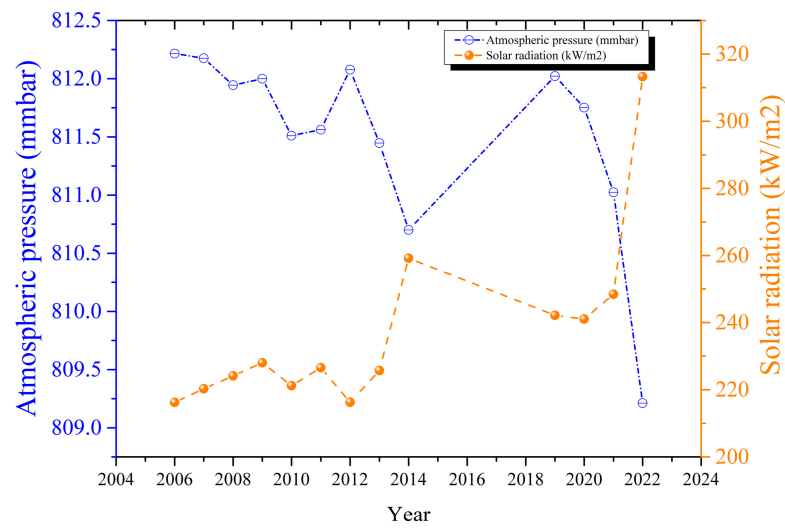


Figure 4. Atmospheric pressure and solar radiation in Morelia, Michoacan, México.

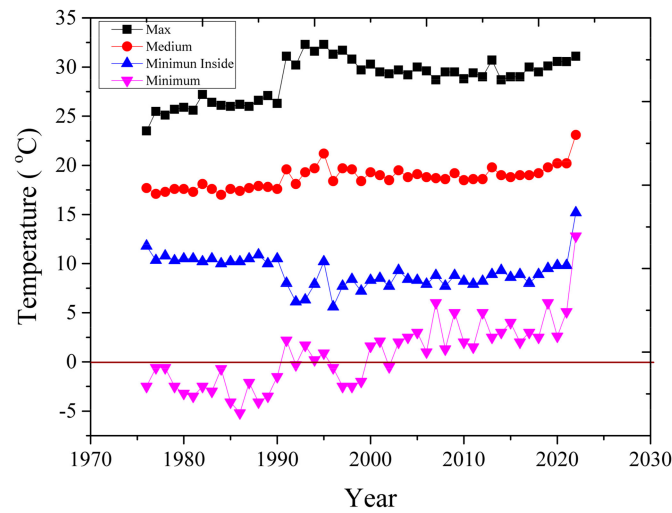


Figure 5. Temperature in Morelia, Michoacan, México.

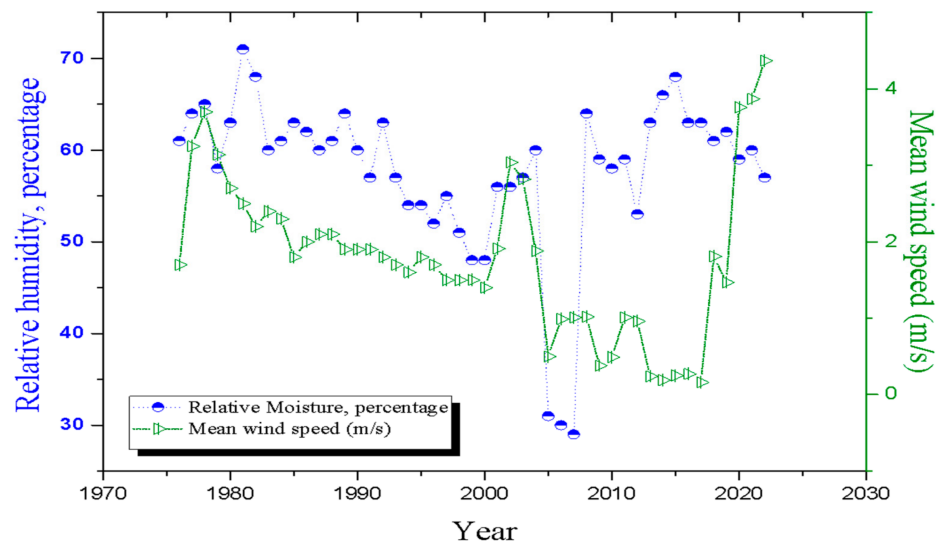


Figure 6. Average wind speed and relative humidity percentage in Morelia, Michoacan, México.

2.3. Methodology

The research carried out on the historical monuments was of the experimental type through the application of field and laboratory tests. For sclerometry, measurements were taken directly in the buildings. To obtain their microstructure, fragments or chips were obtained from the monuments under study donated by the local government and/or ecclesiastical authorities. For the study of ignimbrite banks, candidates to serve as suppliers of healthy rocks for potential conservation and restoration of the historic buildings of Morelia, ignimbrite specimens were sampled and obtained from quarries in the surroundings of Morelia: Cointzio (Coin), Jamaica (Jam), and Tejocote (Tej). The fieldwork consisted of visual identification of damage and possible interpretation of the causes of pathologies. Furthermore, non-destructive testing, such as sclerometry, was useful to qualitatively determine the structural integrity of the stones and the mechanical characteristics in situ.

Other tests performed were: absorption, density, and specific gravity (ASTM C97/C97M-18); mechanical tests such as uniaxial compressive strength (UCS) on cubic samples (ASTM C170/C170M-17) and by sclerometry (ASTM D5873-14); and microstructural observations, according to the corresponding standards [80–82]. Samples of environmentally damaged ignimbrite and healthy ignimbrite samples from quarries currently in use were analyzed by X-ray diffraction (XRD) and X-ray fluorescence (XRF), using the X-ray diffractometer models D5000 and ANDREA H, respectively. These analyzes were made at the National Laboratory of Sciences for Research and Conservation of Cultural Heritage (LANCIC) in México City. In addition, samples were obtained for microstructural observation with scanning electron microscopy (SEM) with equipment JEOL model JSM-6400 of the Institute for Research in Metallurgy and Materials in Morelia, México.

In relation to mechanical compressive strength, there are different indirect methods to determine the so-called “uniaxial compressive strength” (UCS) of rocks; in one of them, the estimation of UCS is based on the rebound value of the Schmidt hammer [83].

Uniaxial compression strength (UCS) tests were performed directly on cubic specimens (5 cm × 5 cm × 5 cm). However, the standard test for the determination of rock hardness using the rebound hammer method (Figure 7) was very important because it was possible to obtain the uniaxial compressive strength directly from the monument in the different environmentally damaged facades (north, south, east, and west) that constitute the historic buildings of this study. UCS can be calculated based on the following equation:

$$UCS = 0.004HS_L^{2.5972} \quad (1)$$

where UCS is uniaxial compressive strength, and HS_L is the rebound number of the Schmidt hammer [84].

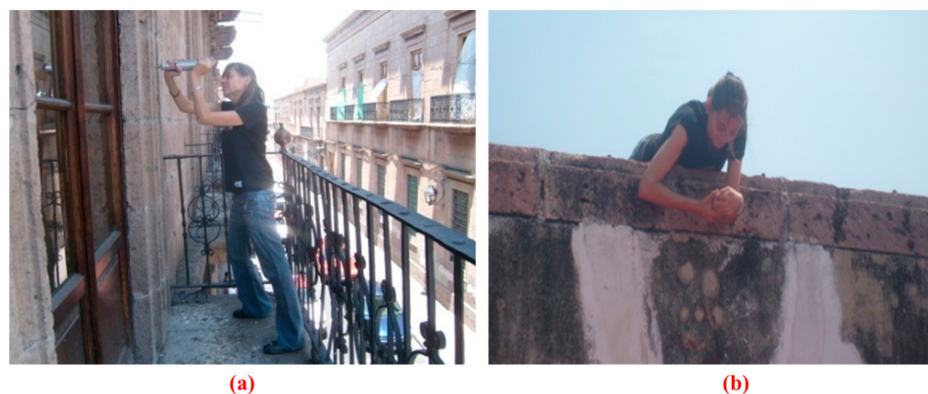


Figure 7. (a) Sclerometer or Schmidt hammer and (b) the test with the sclerometer at the Regional Museum of Michoacan (MR).

For the estimation of the UCS in the monuments studied, five test readings were taken at each point of the sampled surface, with the procedure being repeated at heights of 0.5 m,

1.0 m, and 1.5 m above the sidewalk level in each building, using a Schmidt hammer (James Instrument-NDT, W-M-255 Low Impact Manual Sclerometer). Subsequently, when the corresponding report was produced, the average was obtained to verify the accuracy of each reading. The rebound value test for all historic buildings (CAT, CC, CAP, SAN, and MR) yielded 1713 data in total. The data reported are the average of five readings, and the data did not present variations of $\pm 10\%$.

3. Results and Discussions

Damage begins with a change in the appearance of the ignimbrite surface. Regularly, a darker tonality is produced by pollutants in the atmosphere, black crust, and the wetting–drying process to which the ignimbrites are exposed. Several historical monuments have stains due to humidity on their facades, approximately between 2.0 and 2.5 m above the level of the sidewalk (Figure 8). The humidity is due to the existing water in the soil of the foundation, which by capillarity, is absorbed by the rocks that form the walls.



Figure 8. (a) The south facade of the cathedral (CAT), (b) the north facade of Capuchinas church (CAP), (c) the east and north facades of the Regional Museum of Michoacan (MR), and (d) the south and east facades of the Temple of the Carmen (CC).

The existing damage, generated gradually over the years, begins with a change in the appearance of the surface (Figure 9a), detachment of the material in the form of fragments, shards, flakes, and powders (Figure 9a,b), the loss of the mortar that joins the ignimbrites (Figure 9c), and the presence of flora in the mortar that joins the stones (Figure 9d). In addition, there is friction damage caused by humans in the main entrances of the temples, causing significant loss of ignimbrites (Figure 9b). In some facades, human waste was observed at the ground level (Figure 9c), and the presence of lichens in the upper parts because of the accumulation of water and humidity, gradually causing the degradation of the ignimbrite at the surface level (Figure 9e). Graffiti was also found as part of the vandalism of the historical monuments. The mechanical abrasion method is used to remove them regularly, generating greater damage to the ignimbrite surface (Figure 9f).

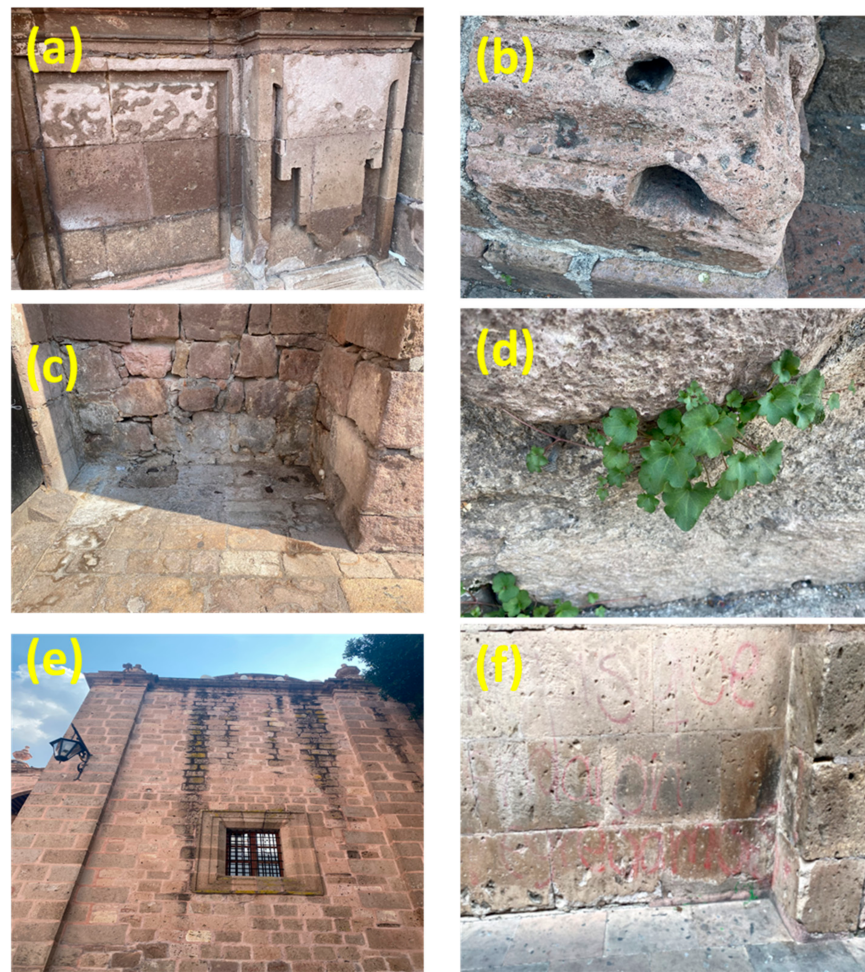


Figure 9. Common forms of deterioration in the facades of historical monuments: (a) weathering of ignimbrites at the surface level, (b) damage due to contour scaling and deeper damage to ignimbrites, (c) loss of mortar between ignimbrite blocks, (d) flora at the surface level of the facades, (e) lichens on the highest parts of the facades, and (f) graffiti.

It is evident that there is deterioration in the buildings studied in this research; the damage is mainly in the lower zone of the facades, in the stones, and in the mortar that joins them. It was found in the altered samples of the different historic buildings and healthy rocks that there is a presence of silica (SiO_2), quartz (SiO_4), and albite, among other mineral particle compounds from each sample (Figure 10). According to the mineralogy of the SAN samples, the matrix is a greenish-brown glass with abundant recrystallization points and incipient appearance of chalcedony, containing small plagioclase microlites, pyroxenes transformed to magnetite or antigorite. The Capuchinas church (CAP) sample also presents a dark greenish matrix containing fragments of minerals and lithics of basaltic composition; in some parts of it, there is chalcedony and the punctual replacement of calcite. The few lithics it contains present an andesitic composition with plagioclase (Andesine) and pyroxenes (Augite) that, in some cases, are chloritized or transformed to antigorite. The ignimbrites are mainly composed of rhyolite [70].

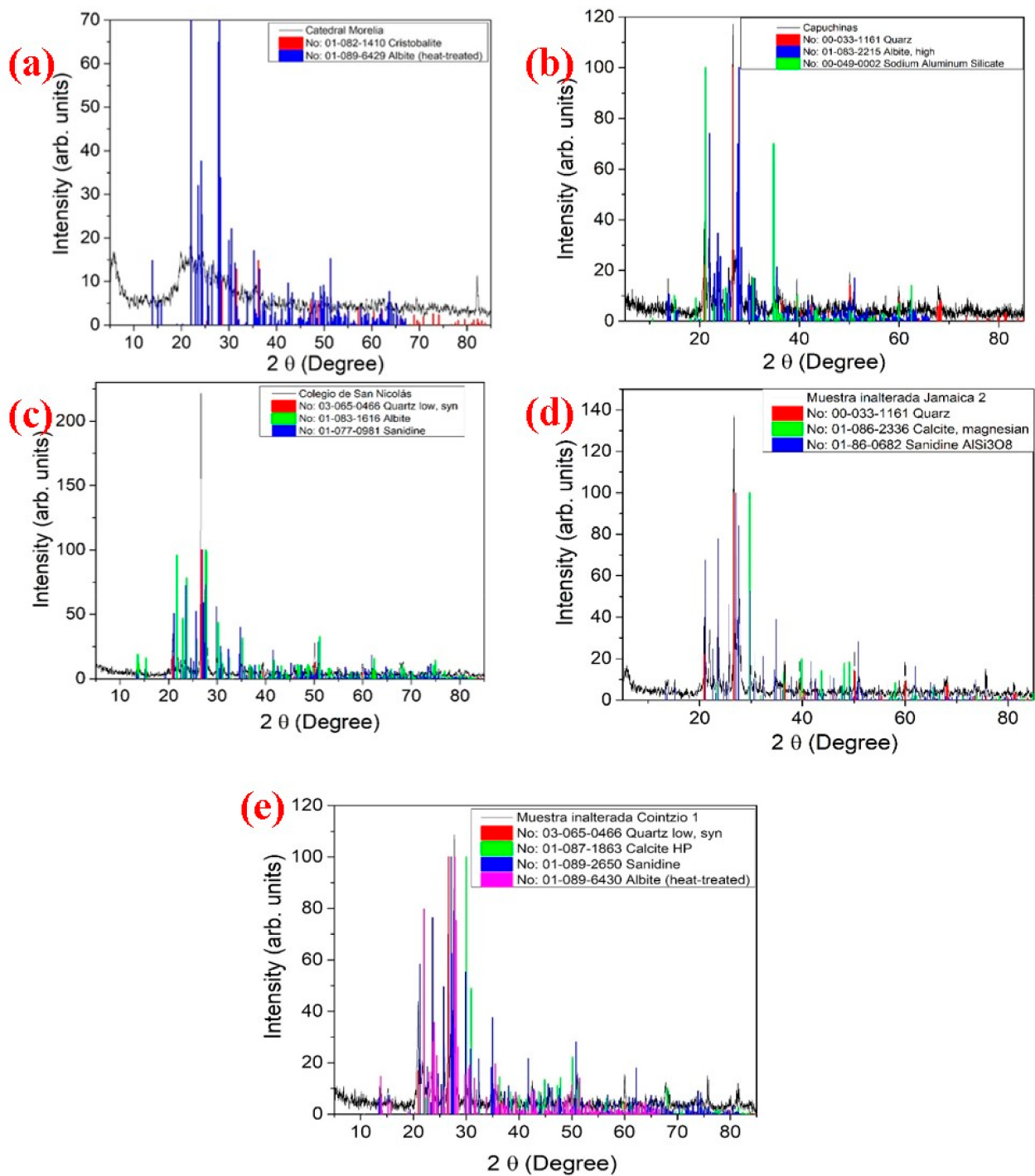


Figure 10. The ignimbrite shards were ground until mesh 400 ASTM. Diffractograms: (a) CAT, (b) CAP, (c) SAN, (d) Jamaica (Jam), and (e) Cointzio (Coin).

With the analytical technique of X-ray fluorescence, the chemical composition of the rocks was determined, with it finding that the historic buildings were built with very similar ignimbrites, and this is demonstrated in Figure 11, where the average percentage of SiO_2 is in a range between 71.6% and 75.1%. A very similar trend in chemical composition (TiO_2 , Al_2O_3 , F_2O_3 , MnO , MgO , CaO , Na_2O , K_2O , and P_2O_5) is evident, so there is homogeneity in the composition of the samples analyzed, since the ignimbrites come from the same magmatic event of the Mexican Volcanic Belt.

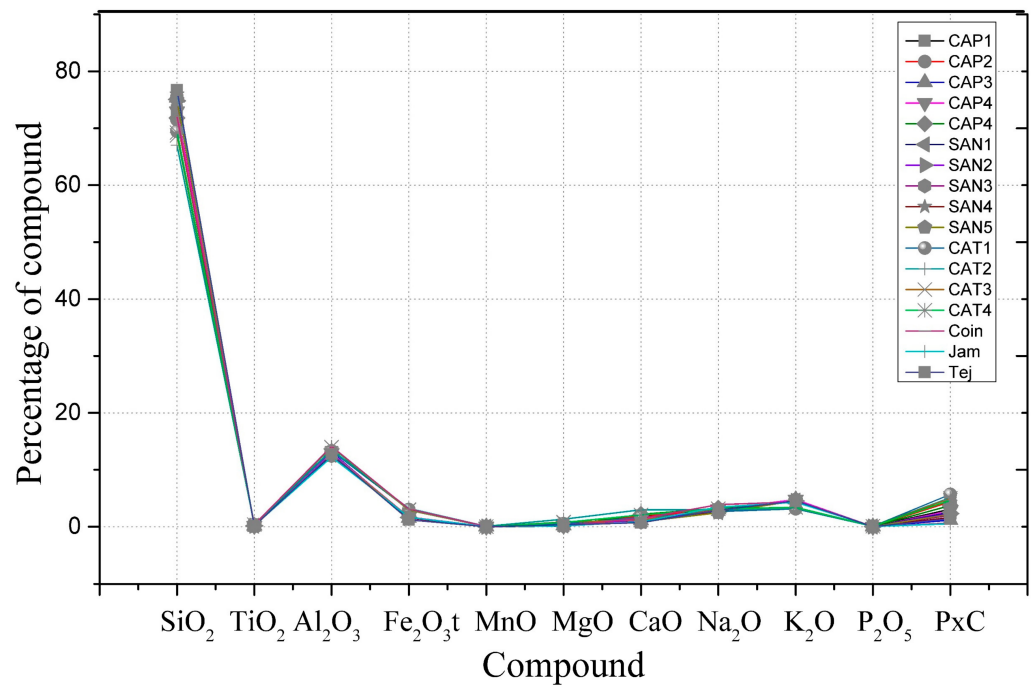


Figure 11. X-ray fluorescence in the samples from the historic buildings and the samples from the quarries.

In the photomicrograph of the CAT sample (Figure 12a), there is a crystal composition with different shapes and dimensions, its grains have a large surface area, and the topography is irregular. In the SAN sample (Figure 12b), the grains are very close together, and its surface is compact with the presence of crystals and flakes of different sizes. The CAT and SAN samples come from the balustrade and the ribs of the dome, respectively, showing how the environment damaged and metamorphosed them, especially by the prevailing winds because they were at average heights of 50 m and the ignimbrite blocks of the lower parts are where the rain splashes occur, cleaning exhaust from motor vehicles. The monuments lasted decades in their construction, and the blocks came from different attack fronts or from different quarries around, which is observed in the different constructive strata, but in general terms, they are very similar.

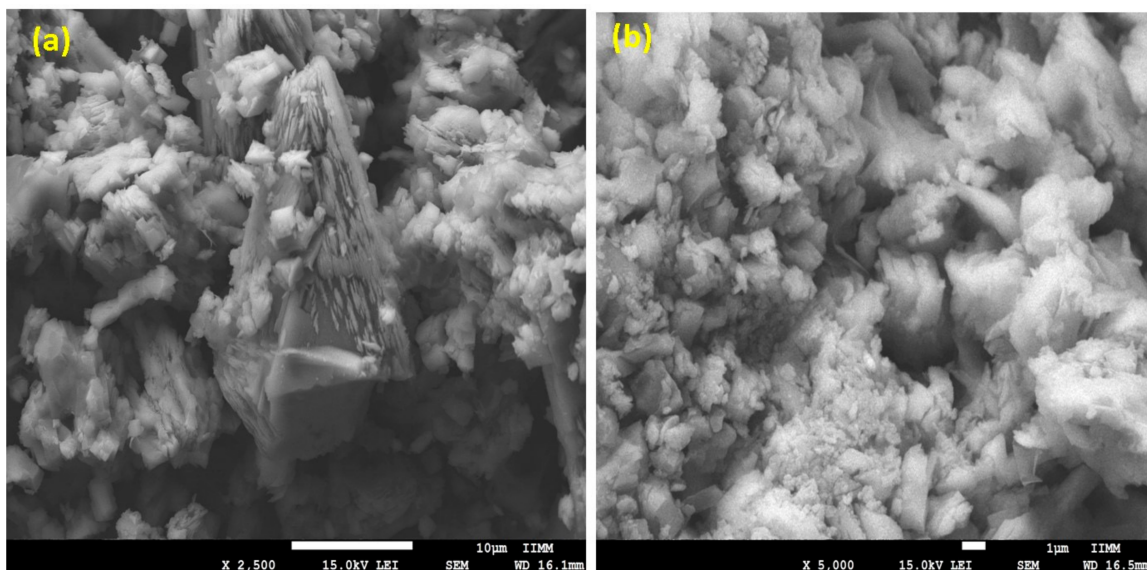


Figure 12. Scanning electron microscopy (SEM): (a) CAT south facade balustrade and (b) SAN.

These characteristics found by SEM analysis allow us to infer that they are the product of the influence of pollutants, as shown in Figure 2a,b. It is clear that there are SO₂ emissions of which there is evidence in microphotographs (Figure 13a,b) that are known as environmental particles, in this case, with the presence of sulfur [85]. However, the presence of carbon monoxide produced by the incomplete combustion of fuels in the vehicle fleet of the city of Morelia is also observed.

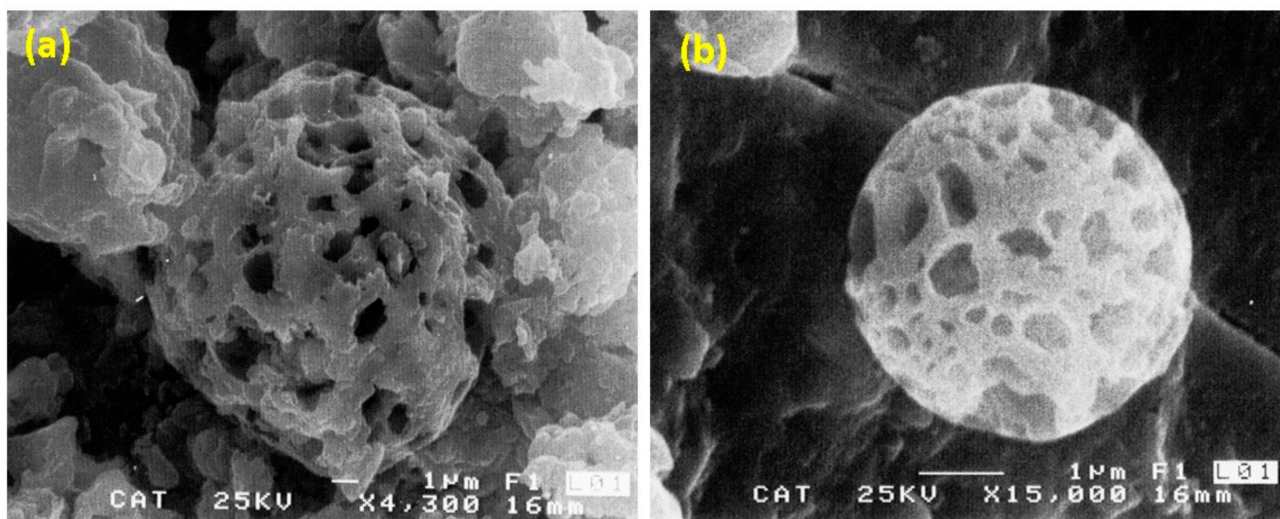


Figure 13. (a,b) Environmental particles that form the patinas on the cathedral's balustrade (CAT).

The results of the physical and mechanical tests are shown in Figure 14. In the rocks studied, mechanical compressive strength is proportional to both bulk density and specific gravity (volumetric mass) and inversely proportional to water absorption. In addition, the UCS values of recently excavated sound quarries (Coin, Jam, and Tej) vary from 40 to 100 kg/cm² compared to those located in historic buildings (CC, CAP, SAN, and CAT), which range from 290 to 350 kg/cm² made in rock cubes.

Some limits suggested by recent construction standards that are generally applied in civil works are also shown. This serves as a parameter that allows understanding the physical and mechanical behavior of the ignimbrites with which the historic buildings were constructed, but these standards cannot be applied in the restoration of historical monuments because ignimbrites with similar properties to those originally constructed are required. It was observed that the ignimbrite quarries (Coin, Jam, and Tej) are below the values of the physical and mechanical properties required for the restoration of historical monuments.

To determine the damage to the historic buildings, their uniaxial compressive strength was obtained by means of a sclerometer or a Schmidt hammer at heights of 0.5 m, 1 m, and 1.5 m on each of the facades of the five historic buildings studied. The study was carried out according to the orientation of the north, south, east, and west facades, but some historic buildings do not adjoin some avenues or streets and therefore do not have the four facades.

The box-plot diagrams (Figure 15) show the values of the rebound performed with the Schmidt hammer and provide information such as measures of central tendency and data dispersion around the median. In addition, it can be observed that the rebound number value (HS_L) ranges from 29 to 48.3. The rocks with which the historic buildings were constructed have a different hardness among them because of the damage generated over the years. However, there are some overlaps as CC and CAT have very similar rebound values. The historic building MR has higher rebound values compared to CC, CAT, CAP, and SAN, with the values of the studied banks of Cointzio (Coin), Jamaica (Jam), and Tejocote (Tej) being well below the estimated UCS value of the studied buildings.

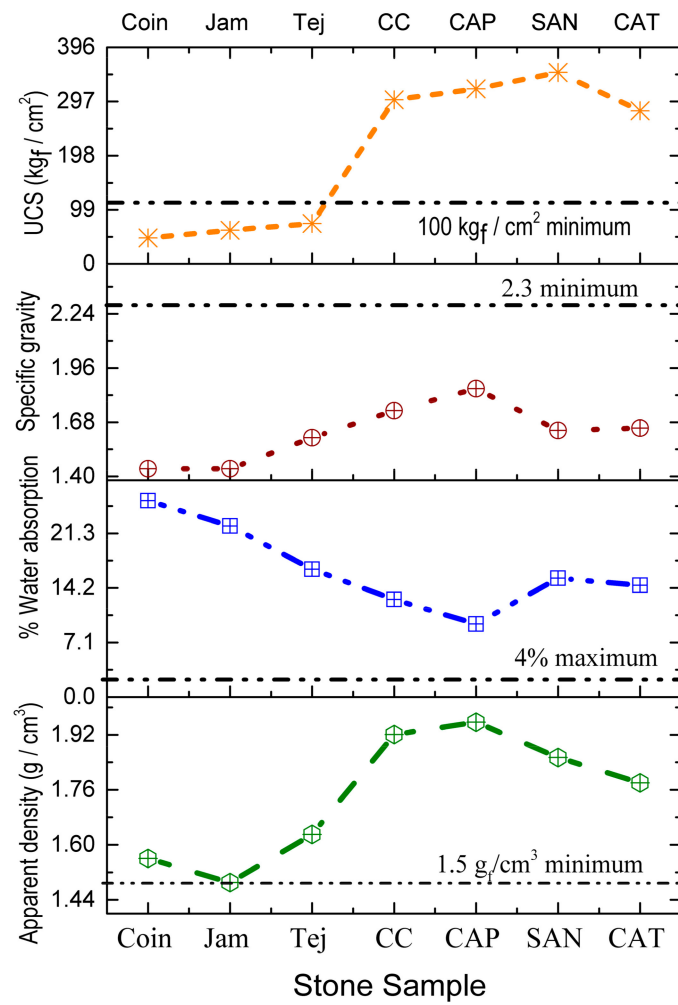


Figure 14. Physical and mechanical tests.

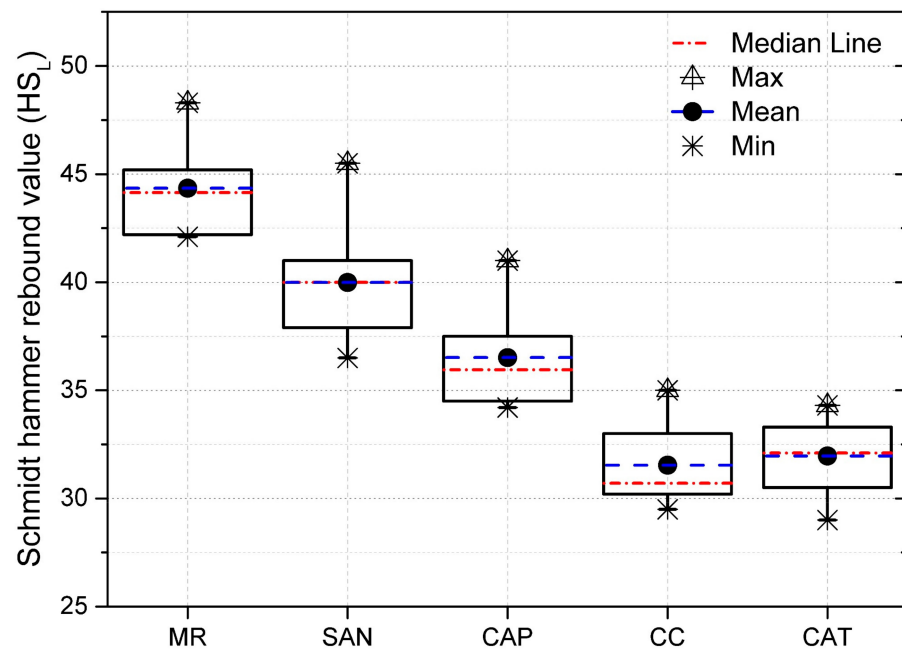


Figure 15. Statistics of the rebound value of the Schmidt hammer for all orientations (north, south, east, and west).

Figure 16 shows that the south-facing facades with the lowest UCS index resistance are CC and CAT. It is important to keep in mind that not all buildings have south facades in the historic center. As for the east- and south-facing facades, very similar resistances were recorded, coincidentally in the same historic buildings: CC and CAT. However, the west- and north-facing facades show higher resistances than the south- and east-facing ones, with this being more evident in the decrease in resistance in the south facade of CAT, as shown in Figure 17.

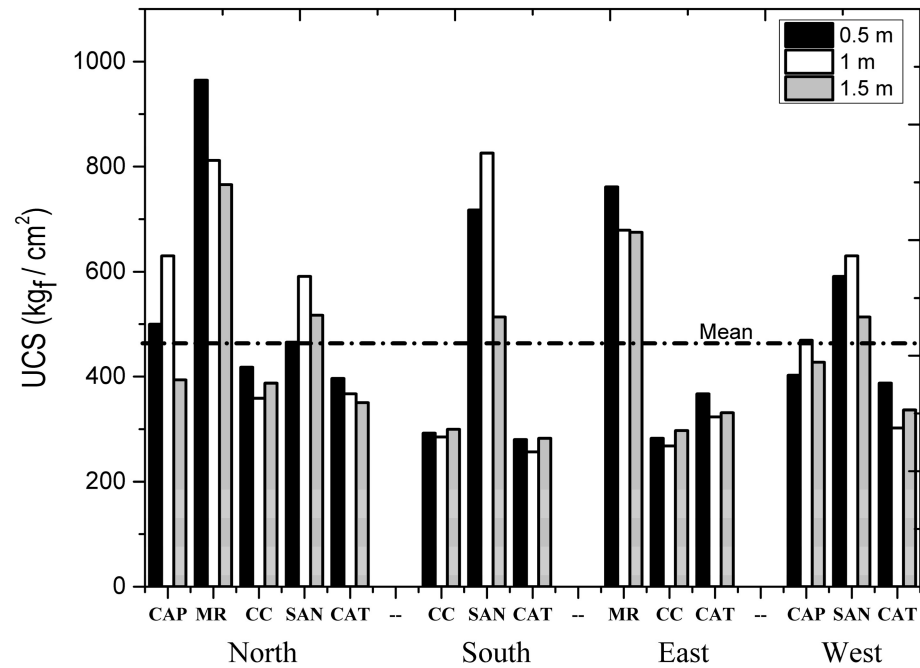


Figure 16. UCS of all the facades of the monuments studied.

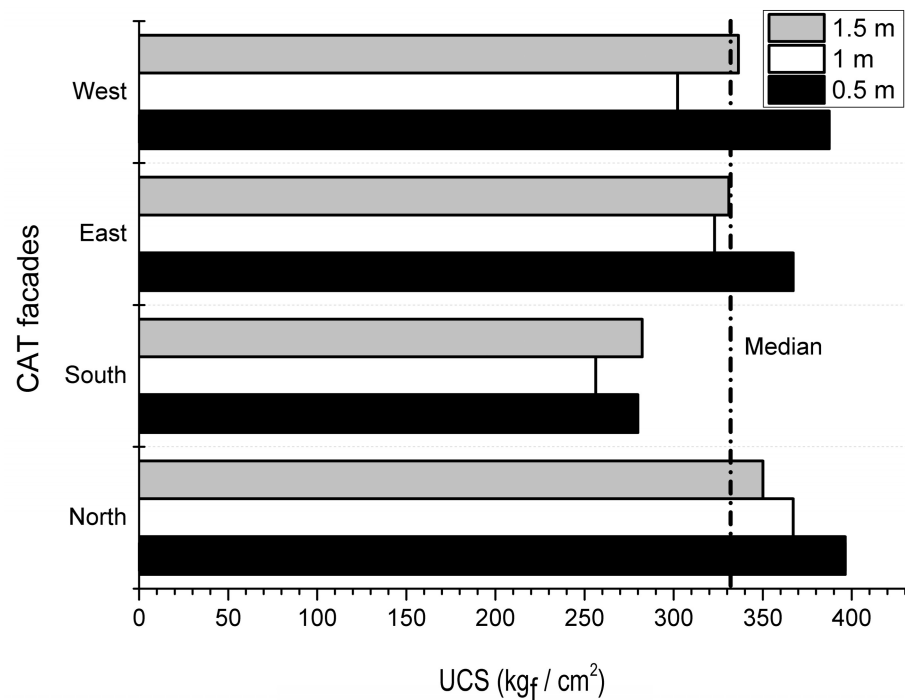


Figure 17. Comparison of the UCS of CAT by facade.

Figure 16 shows that the UCS of historical monuments is diminished on the facades that coincide with the prevailing winds, which reportedly come from the southeast for most of the year. In addition, pollutant emissions due to vehicular traffic, the width of roads, and climatic conditions such as precipitation, solar radiation, wind speed, temperature, and relative humidity are also agents that intensify the deterioration process of the rocks of heritage buildings.

A mathematical model was obtained to estimate the UCS based on the results of sclerometry at heights of 0.5 m, 1.0 m, and 1.5 m above the bench level. With this correlation, it is observed that despite the ignimbrites being damaged at the surface level in their different orientations (north, south, east, and west), it is once again demonstrated that the ignimbrites used in the construction of the historic buildings come from the same geological origin since the correlation coefficient R^2 equal to 0.9086 is excellent (Figure 18).

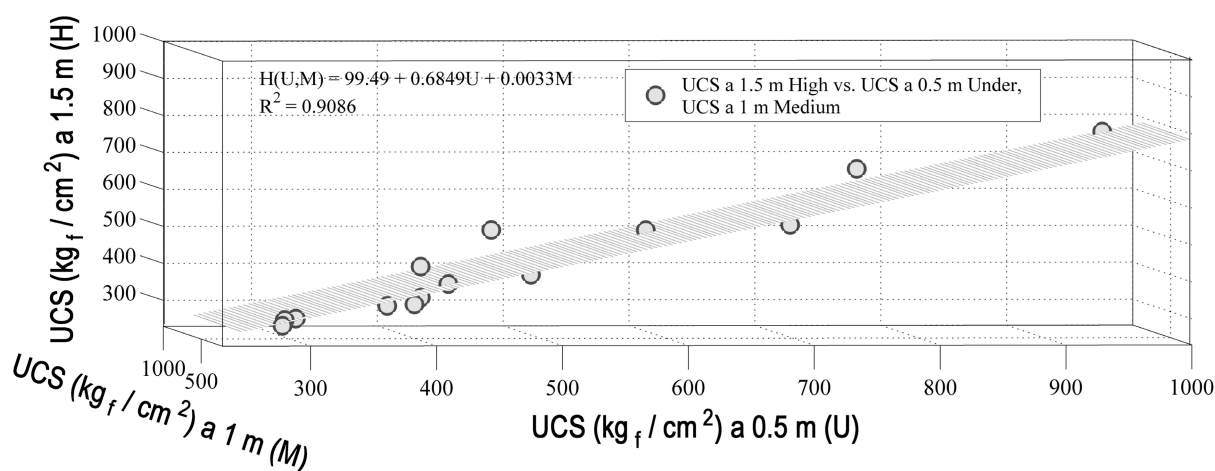


Figure 18. Correlation of the uniaxial compressive strength (UCS) at the heights of 0.5 m, 1 m, and 1.5 m above the level of the sidewalk of the five buildings (north, south, east, and west facades).

The logistic classification is a statistical method of binary classification that, in this research, allows for observation of the resistances from 0.5 m to 1 m and from 0.5 m to 1.5 m. The decision boundary, which is the blue line delimits the existence of higher damage at the height of 1.5 m for the facades with higher UCS (MR, SAN, and CAP) and higher damage for the facades with lower UCS (CC and CAT) at the height of 1.0 m (Figure 19). This can be proven by Figure 8c, where it is shown that the greater damage in the MR monument occurs above 1.5 m, while in the cathedral (CAT) occurs around 1.0 m. However, there is some damage at a height below 0.5 m at the focal points of the different facades, such as the loss of ignimbrite surfaces (Figure 9). UCS values for the different historic buildings are also observed, where the clearest difference is presented when comparing the regional museum (MR) and the cathedral (CAT), which present the highest and lowest UCS values, respectively.

The studies shown above indicate that there is deterioration in the historical heritage of Morelia, generated by atmospheric contamination and intensified by the climatic conditions present. This is manifested by an evident change in the appearance of the ignimbrite (flaking, efflorescence, discoloration, spalling, and black crusting) that translates into a loss of uniaxial compressive strength. Although there are recently excavated ignimbrite quarries (Coin, Jam, and Tej), their physical and mechanical properties are inferior to those of the rocks with which the historic buildings were constructed (Figure 14). Therefore, work must be carried out to preserve their heritage and to continue exploring and studying rock banks that have similar properties to the rocks of the monuments studied to continue repairing the damage and preserving their splendor.

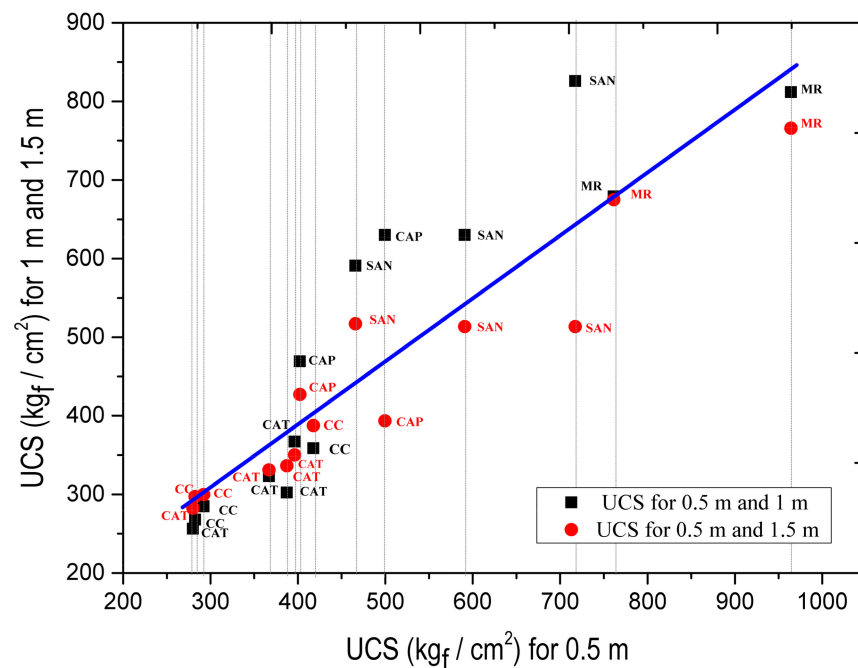


Figure 19. Logistic classification of UCS comparing the resistances at 0.5 m with 1 m and 0.5 m with 1.5 m.

4. Conclusions

Damage to the rocks that make up the walls of the facades of buildings can be divided into lower damage, located from the sidewalk level up to an average height of 2.50 m, and upper damage, from 2.50 m to the top of the facades. The damage in the interior is mainly caused by the emission of polluting vehicular gases, products of the inefficient burning of fuel; by the capillary water that, in the rainy season, ascends the walls and deposits salts in the pores of the rocks, drying up in the dry season but causing the same phenomenon annually; and by the actions of humans who injure the monuments in conscious or unconscious ways. Graffiti, enamel paint, oil stains, and human waste are degradation factors, as are scratches, blows, friction damage caused by people at building entrances, stains, and inadequate repair interventions, mainly those using Portland-cement-based mortars. Carelessness on the part of building owners, the government, or private individuals is another factor that hinders the conservation and restoration of historical monuments. In addition, climatic factors influence the degradation of the rocks. However, it is maintained that it mainly affects the upper part of the facades, above the capillary water level mentioned above. Damage to the upper parts of the facades is mainly caused by environmental contaminants, accelerating the weathering of the rocks. The south- and west-facing facades suffer greater deterioration due to the prevailing southwesterly winds, which transport and deposit pollutants on the rocks, as well as the incidence of solar radiation, which has a greater impact on this orientation. Pigeon droppings significantly damage rocks due to their acidity, with a pH between 4.5 and 5.0, in addition to the fact that they favor the growth of vascular plants, which cause mechanical deterioration of the rocks through the penetration and growth of their roots.

The compressive strength of the rocks of the studied facades was determined with a sclerometer, obtaining a lower resistance in the facades exposed to denser vehicular traffic and facades oriented to the prevailing winds and in streets with smaller widths. The mineralogical study indicated that the ignimbrites of the historical monuments are composed of andesite; the dark greenish color and the transformation to antigorite confirm that there is deterioration produced by adverse climatic conditions and contaminating agents generated by the use of fossil fuels in motor vehicles and public transportation units. The UCS in the

lower zone of the different facades oscillates between 290 kg_f/cm² and 350 kg_f/cm², which reaffirms the damage suffered by the ignimbrites and their gradual weathering.

To reduce the damage to architectural heritage caused by environmental contamination, it is pertinent to identify preventive and corrective measures. Some of these measures include the partial restriction of public transportation in the historic center of Morelia, the use of sacrificial coatings (mortars) that impede direct contact between the different agents of deterioration and the ignimbrites, and the search for quarries that meet the physical-mechanical characteristics of the ignimbrites used in historical monuments since the present work shows that the current quarries do not achieve this.

The present study demonstrates that the ignimbrites of the monuments directly exposed to weathering and anthropogenic activity are losing mechanical resistance, which entails strong implications for structural safety, as well as the proliferation of different pathologies that will make future conservation work difficult. This highlights the urgent need to create conservation and restoration protocols based on technical-scientific information that will provide certainty to decision-makers in this area and help to raise awareness among users of these historical monuments.

Author Contributions: Conceptualization, R.R.-R. and E.M.A.-G.; methodology, R.R.-R., E.M.A.-G., M.A.N.-S., W.M.-M. and M.A.-S.; software, M.A.N.-S., J.A.B.-P. and L.A.M.-R.; validation, R.R.-R., J.A.V.-P. and L.A.M.-R.; formal analysis, E.M.A.-G., W.M.-M. and H.L.C.-G.; investigation, J.A.B.-P. and M.A.N.-S.; resources, E.M.A.-G.; writing—original draft preparation, E.M.A.-G., R.R.-R., M.A.-S. and J.A.B.-P.; writing—review and editing, M.A.-S. and R.R.-R.; visualization, L.A.M.-R. and H.L.C.-G.; supervision, E.M.A.-G. and W.M.-M.; project administration, H.L.C.-G. and W.M.-M. All authors have read and agreed to the published version of the manuscript.

Funding: This research received no external funding.

Data Availability Statement: Data are contained within the article.

Acknowledgments: The authors would like to acknowledge sponsorship from: CIC Projects at Universidad Michoacana de San Nicolas de Hidalgo, UMSNH; the National Council of Science and Technology, CONACYT; Project 321260: Development of a replicable social production model for housing and habitat.; SEP-Prodep; Laboratory “Ing. Luis Silva Ruelas”, Faculty of Civil Engineering, UMSNH; and the Institute of Science, Technology, and Innovation, ICTI.

Conflicts of Interest: The authors declare no conflict of interest.

References

1. Sengun, N.; Demirdag, S.; Akbay, D.; Ugur, İ.; Altindag, R.; Akbulut, A. Investigation of the relationships between capillary water absorption coefficients and other rock properties of some natural stones. In Proceedings of the V Global Stone Congress, Antalya, Turkey, 22–25 October 2014.
2. İnce, İ. Relationship Between Capillary Water Absorption Value, Capillary Water Absorption Speed, and Capillary Rise Height in Pyroclastic Rocks. *Mining Metall. Explor.* **2021**, *38*, 841–853. [[CrossRef](#)]
3. Alves, C.; Figueiredo, C.; Sanjurjo-Sánchez, J. Rock features and alteration of stone materials used for the built environment: A review of recent publications on ageing tests. *Geoscience* **2020**, *10*, 91. [[CrossRef](#)]
4. Sardella, A.; Palazzi, E.; von Hardenberg, J.; Del Grande, C.; De Nuntiis, P.; Sabbioni, C.; Bonazza, A. Risk Mapping for the Sustainable Protection of Cultural Heritage in Extreme Changing Environments. *Atmosphere* **2020**, *11*, 700. [[CrossRef](#)]
5. Sitzia, F. Climate Change and Cultural Heritage: From Small- to Large-Scale Effects—The Case Study of Nora (Sardinia, Italy). *Heritage* **2022**, *5*, 3495–3514. [[CrossRef](#)]
6. Striani, R.; Cappai, M.; Casnedi, L.; Esposito Corcione, C.; Pia, G. Coating’s influence on wind erosion of porous stones used in the Cultural Heritage of Southern Italy: Surface characterisation and resistance. *Case Stud. Constr. Mater.* **2022**, *17*, e01501. [[CrossRef](#)]
7. Richards, J.; Zhao, G.; Zhang, H.; Viles, H. A controlled field experiment to investigate the deterioration of earthen heritage by wind and rain. *Herit. Sci.* **2019**, *7*, 1–13. [[CrossRef](#)]
8. Grau-Bové, J.; Mazzei, L.; Strlic, M.; Cassar, M. Fluid simulations in heritage science. *Herit. Sci.* **2019**, *7*, 1–12. [[CrossRef](#)]
9. Olenkov, V.; Puzyrev, P. Study of Wind Effects on Unique Buildings. *IOP Conf. Ser. Mater. Sci. Eng.* **2017**, *262*. [[CrossRef](#)]
10. Wang, X.; Meng, J.; Zhu, T.; Zhang, J. Prediction of Wind Erosion over a Heritage Site: A Case Study of Yongling Mausoleum, China. *Built Herit.* **2019**, *3*, 41–57. [[CrossRef](#)]
11. Germinario, L.; Coletti, C.; Girardi, G.; Maritan, L.; Praticelli, N.; Sassi, R.; Solstad, J.; Mazzoli, C. Microclimate and Weathering in Cultural Heritage: Design of a Monitoring Apparatus for Field Exposure Tests. *Heritage* **2022**, *5*, 3211–3219. [[CrossRef](#)]

12. Michette, M.; Viles, H.; Vlachou, C.; Angus, I. Do environmental conditions determine whether salt driven decay leads to powdering or flaking in historic Reigate Stone masonry at the Tower of London? *Eng. Geol.* **2022**, *303*, 106641. [[CrossRef](#)]
13. López-González, L.; Gomez-Heras, M.; Otero-Ortiz de Cosca, R.; Garcia-Morales, S.; Fort, R. Coupling electrical resistivity methods and GIS to evaluate the effect of historic building features on wetting dynamics during wind-driven rain spells. *J. Cult. Herit.* **2022**, *58*, 209–218. [[CrossRef](#)]
14. Celik, M.Y.; Kacmaz, A.U. The investigation of static and dynamic capillary by water absorption in porous building stones under normal and salty water conditions. *Environ. Earth Sci.* **2016**, *75*. [[CrossRef](#)]
15. Al-Naddaf, M. A new automatic method for continuous measurement of the capillary water absorption of building materials. *Constr. Build. Mater.* **2018**, *160*, 639–643. [[CrossRef](#)]
16. Tomašić, I.; Lukić, D.; Peček, N.; Kršinić, A. Dynamics of capillary water absorption in natural stone. *Bull. Eng. Geol. Environ.* **2011**, *70*, 673–680. [[CrossRef](#)]
17. Karagiannis, N.; Karoglou, M.; Bakolas, A.; Krokida, M.; Moropoulou, A. Drying kinetics of building materials capillary moisture. *Constr. Build. Mater.* **2017**, *137*, 441–449. [[CrossRef](#)]
18. Ruedrich, J.; Siegesmund, S. Salt and ice crystallisation in porous sandstones. *Environ. Geol.* **2007**, *52*, 225–249. [[CrossRef](#)]
19. Lezzerini, M.; Tomei, A.; Gallelo, G.; Aquino, A.; Pagnotta, S. The Crystallization Effect of Sodium Sulfate on Some Italian Marbles, Calcarenites and Sandstones. *Heritage* **2022**, *5*, 1449–1461. [[CrossRef](#)]
20. Cowell, D.; Apsimon, H. Estimating the cost of damage to buildings by acidifying atmospheric pollution in Europe. *Atmos. Environ.* **1996**, *30*, 2959–2968. [[CrossRef](#)]
21. Leygraf, C.; Wallinder, I.O.; Tidblad, J.; Graedel, T. *Atmospheric Corrosion*, 2nd ed.; Wiley: Hoboken, NJ, USA, 2016.
22. Newby, P.T.; Mansfield, T.A.; Hamilton, R.S. Sources and economic implications of building soiling in urban areas. *Sci. Total Environ.* **1991**, *100*, 347–365. [[CrossRef](#)]
23. Rabl, A. Air pollution and buildings: An estimation of damage costs in France. *Environ. Impact Assess. Rev.* **1999**, *19*, 361–385. [[CrossRef](#)]
24. Watt, J.; Tidblad, J.; Hamilton, R.; Kucera, V. *The Effects of Air Pollution on Cultural Heritage*; Springer: Berlin/Heidelberg, Germany, 2009.
25. Bonazza, A.; Sabbioni, C.; Ghedini, N. Quantitative data on carbon fractions in interpretation of black crusts and soiling on European built heritage. *Atmos. Environ.* **2005**, *39*, 2607–2618. [[CrossRef](#)]
26. Barca, D.; Comite, V.; Belfiore, C.M.; Bonazza, A.; La Russa, M.F.; Ruffolo, S.A.; Crisci, G.M.; Pezzino, A.; Sabbioni, C. Impact of air pollution in deterioration of carbonate building materials in Italian urban environments. *Appl. Geochem.* **2014**, *48*, 122–131. [[CrossRef](#)]
27. Liu, D.; Guo, X.; Xiao, B. What causes growth of global greenhouse gas emissions? Evidence from 40 countries. *Sci. Total Environ.* **2019**, *661*, 750–766. [[CrossRef](#)]
28. Patrón, D.; Lyamani, H.; Titos, G.; Casquero-Vera, J.A.; Cardell, C.; Močnik, G.; Alados-Arboledas, L.; Olmo, F.J. Monumental heritage exposure to urban black carbon pollution. *Atmos. Environ.* **2017**, *170*, 22–32. [[CrossRef](#)]
29. Spezzano, P. Mapping the susceptibility of UNESCO World Cultural Heritage sites in Europe to ambient (outdoor) air pollution. *Sci. Total Environ.* **2021**, *754*, 142345. [[CrossRef](#)]
30. Alonso, E.; Martínez, L. The role of environmental sulfur on degradation of ignimbrites of the Cathedral in Morelia, Mexico. *Build. Environ.* **2003**, *38*, 861–867. [[CrossRef](#)]
31. Monforti, F.; Bellasio, R.; Bianconi, R.; Clai, G.; Zanini, G. An evaluation of particle deposition fluxes to cultural heritage sites in Florence, Italy. *Sci. Total Environ.* **2004**, *334–335*, 61–72. [[CrossRef](#)]
32. Nava, S.; Becherini, F.; Bernardi, A.; Bonazza, A.; Chiari, M.; García-Orellana, I.; Lucarelli, F.; Ludwig, N.; Migliori, A.; Sabbioni, C.; et al. An integrated approach to assess air pollution threats to cultural heritage in a semi-confined environment: The case study of Michelozzo's Courtyard in Florence (Italy). *Sci. Total Environ.* **2010**, *408*, 1403–1413. [[CrossRef](#)]
33. Watt, J.; Jarrett, D.; Hamilton, R. Dose-response functions for the soiling of heritage materials due to air pollution exposure. *Sci. Total Environ.* **2008**, *400*, 415–424. [[CrossRef](#)]
34. Fermo, P.; Comite, V.; Ciantelli, C.; Sardella, A.; Bonazza, A. A multi-analytical approach to study the chemical composition of total suspended particulate matter (TSP) to assess the impact on urban monumental heritage in Florence. *Sci. Total Environ.* **2020**, *740*, 140055. [[CrossRef](#)]
35. Spennemann, D.H.R.; Pike, M.; Watson, M.J. Effects of acid pigeon excreta on building conservation. *Int. J. Build. Pathol. Adapt.* **2017**, *35*, 2–15. [[CrossRef](#)]
36. Prieto, B.; Vázquez-Nion, D.; Fuentes, E.; Durán-Román, A.G. Response of subaerial biofilms growing on stone-built cultural heritage to changing water regime and CO₂ conditions. *Int. Biodeterior. Biodegrad.* **2020**, *148*, 104882. [[CrossRef](#)]
37. Varas-Muriel, M.J.; Fort, R.; Martínez-Garrido, M.I.; Zornoza-Indart, A.; López-Arce, P. Fluctuations in the indoor environment in Spanish rural churches and their effects on heritage conservation: Hygro-thermal and CO₂ conditions monitoring. *Build. Environ.* **2014**, *82*, 97–109. [[CrossRef](#)]
38. Scheerer, S.; Ortega-Morales, O.; Gaylarde, C. Chapter 5 Microbial Deterioration of Stone Monuments-An Updated Overview. *Adv. Appl. Microbiol.* **2009**, *66*, 97–139. [[CrossRef](#)]
39. Farooq, M. Mycobial Deterioration of Stone Monuments of Dharmarajika, Taxila. *J. Microbiol. Exp.* **2015**, *2*, 29–33. [[CrossRef](#)]

40. Vlasov, D.Y.; Frank-Kamenetskaya, O.V.; Manurtdinova, V.V.; Zelenskaya, M.S. *Decay of the Monuments*; Springer: Berlin/Heidelberg, Germany, 2019.
41. Gaylarde, C.C. Influence of environment on microbial colonization of historic stone buildings with emphasis on cyanobacteria. *Heritage* **2020**, *3*, 1469–1482. [[CrossRef](#)]
42. Zhang, Y.; Su, M.; Wu, F.; Gu, J.; Li, J.; He, D.; Guo, Q.; Cui, H.; Zhang, Q.; Feng, H. Diversity and Composition of Culturable Microorganisms and Their Biodeterioration Potentials in the Sandstone of Beishiku. *Microorganisms* **2023**, *11*, 429. [[CrossRef](#)]
43. López-Moreno, A.; Sepúlveda-Sánchez, J.D.; Mercedes Alonso Guzmán, E.M.; Le Borgne, S. Calcium carbonate precipitation by heterotrophic bacteria isolated from biofilms formed on deteriorated ignimbrite stones: Influence of calcium on EPS production and biofilm formation by these isolates. *Biofouling* **2014**, *30*, 547–560. [[CrossRef](#)]
44. García Sáez, M. Biología y Patrimonio Cultural: Estudio de la comunidad de plantas que colonizaban la fachada de la Iglesia de San Pablo (Valladolid). *Ge-Conservación* **2015**, *2015*, 27–36. [[CrossRef](#)]
45. Cozzolino, A.; Adamo, P.; Bonanomi, G.; Motti, R. The Role of Lichens, Mosses, and Vascular Plants in the Biodeterioration of Historic Buildings: A Review. *Plants* **2022**, *11*, 1–19. [[CrossRef](#)] [[PubMed](#)]
46. Lisci, M.; Monte, M.; Pacini, E. Lichens and higher plants on stone: A review. *Int. Biodeterior. Biodegrad.* **2003**, *51*, 1–17. [[CrossRef](#)]
47. Adamo, P.; Violante, P. Weathering of rocks and neogenesis of minerals associated with lichen activity. *Appl. Clay Sci.* **2000**, *16*, 229–256. [[CrossRef](#)]
48. Chen, X.; Bai, F.; Huang, J.; Lu, Y.; Wu, Y.; Yu, J.; Bai, S. The Organisms on Rock Cultural Heritages: Growth and Weathering. *Geoheritage* **2021**, *13*, 56. [[CrossRef](#)]
49. Shirzadian, S.; Uniyal, P.L. Biodeteriorative impacts on bridges over Zayand-e-Rood river (Iran): Role of mosses and their control measures. *J. Sci. Ind. Res.* **2008**, *67*, 377–380.
50. Jang, K.; Viles, H. Moisture Interactions Between Mosses and Their Underlying Stone Substrates. *Stud. Conserv.* **2022**, *67*, 532–544. [[CrossRef](#)]
51. Florian, M.-L. Plant Biology for Cultural Heritage: Biodeterioration and Conservation. *Stud. Conserv.* **2009**, *54*, 191. [[CrossRef](#)]
52. Shrestha, S.; Khanal, L.; Pandey, N.; Kyes, R.C. Conservation of Heritage Sites in Kathmandu, Nepal: Assessing the Corrosion Threat from Pigeon Excreta on Metal Monuments. *Conservation* **2022**, *2*, 233–243. [[CrossRef](#)]
53. Skandrani, Z.; Lepetz, S.; Prévot-Julliard, A.C. Nuisance species: Beyond the ecological perspective. *Ecol. Process.* **2014**, *3*, 3. [[CrossRef](#)]
54. Spennemann, D.H.R.; Watson, M.J. Dietary habits of urban pigeons (*Columba livia*) and implications of excreta pH—A review. *Eur. J. Ecol.* **2017**, *3*, 27–41. [[CrossRef](#)]
55. Spennemann, D.H.; Pike, M.; Watson, M.J. Behaviour of Pigeon Excreta on Masonry Surfaces. *Restor. Build. Monum.* **2018**, *23*, 15–28. [[CrossRef](#)]
56. Lettieri, M.; Masieri, M.; Frigione, M. Durability to simulated bird guano of nano-filled oleo/hydrophobic coatings for the protection of stone materials. *Prog. Org. Coat.* **2020**, *148*, 105900. [[CrossRef](#)]
57. Ben Chobba, M.; Weththimuni, M.L.; Messaoud, M.; Bouaziz, J.; Salhi, R.; De Leo, F.; Urzì, C.; Licchelli, M. Silver-Doped TiO₂-PDMS Nanocomposite as a Possible Coating for the Preservation of Serena Stone: Searching for Optimal Application Conditions. *Heritage* **2022**, *5*, 3411–3426. [[CrossRef](#)]
58. Tesser, E.; Conventi, A.; Majerle, F. Characterization of Barium Hydroxide Used as Consolidating Agent for Monumental Surfaces in Venice. *Heritage* **2022**, *5*, 3280–3297. [[CrossRef](#)]
59. Diz-Mellado, E.; Mascort-Albea, E.J.; Romero-Hernández, R.; Galán-Marín, C.; Rivera-Gómez, C.; Ruiz-Jaramillo, J.; Jaramillo-Morilla, A. Non-destructive testing and Finite Element Method integrated procedure for heritage diagnosis: The Seville Cathedral case study. *J. Build. Eng.* **2021**, *37*, 102134. [[CrossRef](#)]
60. Tejedor, B.; Lucchi, E.; Bienvenido-Huertas, D.; Nardi, I. Non-destructive techniques (NDT) for the diagnosis of heritage buildings: Traditional procedures and futures perspectives. *Energy Build.* **2022**, *263*, 112029. [[CrossRef](#)]
61. Napolitano, R.; Hess, M.; Glisic, B. Integrating Non-Destructive Testing, Laser Scanning, and Numerical Modeling for Damage Assessment: The Room of the Elements. *Heritage* **2019**, *2*, 151–168. [[CrossRef](#)]
62. Pappalardo, G.; Mineo, S.; Caliò, D.; Bognandi, A. Evaluation of Natural Stone Weathering in Heritage Building by Infrared Thermography. *Heritage* **2022**, *5*, 2594–2614. [[CrossRef](#)]
63. Spathis, P.K.; Mavrommati, M.; Gkrava, E.; Tsiroidis, V.; Evgenidis, S.P.; Karapanagiotis, I.; Melfos, V.; Karapantsios, T.D. Characterization of Natural Stone from the Archaeological Site of Pella, Macedonia, Northern Greece. *Heritage* **2021**, *4*, 4665–4677. [[CrossRef](#)]
64. Hiriart Prado, C. El centro histórico de Morelia; un espacio en pugna. La gestión en pro del patrimonio. In *Michoacán: Arquitectura y Urbanismo, Temas Selectos*; UMSNH: Morelia, Mexico, 1999; p. 116.
65. Conaculta. Morelia, Ciudad Patrimonio Mundial. Available online: https://www.cultura.gob.mx/turismocultural/destino_mes/morelia/index.html (accessed on 25 January 2023).
66. Organización de las Ciudades del Patrimonio Mundial (OVPD). Centro Histórico de Morelia. Available online: <https://www.ovpd.org/es/ciudad/morelia-mexico/> (accessed on 8 March 2023).
67. Mercado López, E. *Ideología, Legislación y Patrimonio Cultural*; Secretaría de Cultura de Michoacán: Morelia, Mexico, 2013; ISBN 978-607-8201-44-0.
68. Rodríguez García, J.L. *Patrimonio y Turismo Cultural en Morelia*; UAM: Madrid, Spain, 2001.

69. Hiriart Pardo, C.A. El centro histórico de Morelia (México): Acciones transversales y estrategias para su conservación integral y gestión turística frente a la crisis de inseguridad. In *Personas y Comunidades: Actas del Segundo Congreso Internacional de Buenas Prácticas en Patrimonio Mundial*; Universidad Complutense de Madrid, Servicio de Publicaciones: Madrid, Spain, 2015; pp. 986–1008.
70. Martínez-Martínez, J.; Pola, A.; García-Sánchez, L.; Reyes Agustin, G.; Osorio Ocampo, L.S.; Macías Vázquez, J.L.; Robles-Camacho, J. Building stones used in the architectural heritage of Morelia (México): Quarries location, rock durability and stone compatibility in the monument. *Environ. Earth Sci.* **2018**, *77*, 167. [[CrossRef](#)]
71. SIC. México Catedrales. Available online: https://sic.gob.mx/ficha.php?table=catedral&table_id=46 (accessed on 25 January 2023).
72. Colegio de San Nicolás de Hidalgo. Patrimonio Mundial, Ciudades Mexicanas. Available online: <https://www.ciudadespatrimonio.mx/colegio-de-san-nicolas-de-hidalgo/> (accessed on 25 January 2023).
73. Del Carmen Arguello Hernández, S. Minerales Accesorios Presentes en Ignimbritas, como Resultado de la Meteorización. Ph.D. Thesis, Universidad Michoacana de San Nicolás de Hidalgo, Morelia, Mexico, 2010.
74. SIC. México Museo Regional Michoacano. Available online: https://sic.cultura.gob.mx/ficha.php?table=museo&table_id=1040 (accessed on 25 January 2023).
75. México es Cultura Templo de Nuestra Señora del Carmen. Available online: <https://www.mexicoescultura.com/recinto/68504/templo-de-nuestra-senora-del-carmen.html> (accessed on 25 January 2023).
76. CLIMA. Clima en Morelia. Available online: <https://thewebsitio.es.tl/CLIMA.htm> (accessed on 15 December 2022).
77. National Institute of Ecology and Climate Change. *National Air Quality Report*; National Institute of Ecology and Climate Change: Mexico City, Mexico, 2020.
78. Semarnat Norma Oficial Mexicana. NOM-041-SEMARNAT-2006, Que Establece los Límites Máximos Permisibles de Emisión de Gases Contaminantes Provenientes del Escape de los Vehículos Automotores en Circulación que Usan Gasolina como Combustible. 2015. Available online: <https://www.dof.gob.mx/normasOficiales/1880/SEMARNA/SEMARNA.htm> (accessed on 9 March 2023).
79. Semarnat. Inventarios Nacionales de Emisiones de Contaminantes Criterio. Available online: <https://www.gob.mx/semarnat/documentos/documentos-del-inventario-nacional-de-emisiones> (accessed on 15 December 2022).
80. *ASTM C97/C97M-18*; Standard Test Methods for Absorption and Bulk Specific Gravity of Dimension Stone. ASTM: West Conshohocken, PA, USA, 2018.
81. *ASTM C170/C170M-17*; Standard Test Method for Compressive Strength of Dimension Stone. ASTM: West Conshohocken, PA, USA, 2017.
82. *ASTM D5873-14*; Standard Test Method for Determination of Rock Hardness by Rebound Hammer Method. ASTM: West Conshohocken, PA, USA, 2014.
83. Wang, M.; Wan, W. A new empirical formula for evaluating uniaxial compressive strength using the Schmidt hammer test. *Int. J. Rock Mech. Min. Sci.* **2019**, *123*, 104094. [[CrossRef](#)]
84. Celik, S.B.; Cobanoğlu, İ. Comparative investigation of Shore, Schmidt, and Leeb hardness tests in the characterization of rock materials. *Environ. Earth Sci.* **2019**, *78*, 554. [[CrossRef](#)]
85. Lai Gauri, K.; Holdren, G.C. Pollutant effects on stone monuments. *Environ. Sci. Technol.* **1981**, *15*, 386–390. [[CrossRef](#)] [[PubMed](#)]

Disclaimer/Publisher’s Note: The statements, opinions and data contained in all publications are solely those of the individual author(s) and contributor(s) and not of MDPI and/or the editor(s). MDPI and/or the editor(s) disclaim responsibility for any injury to people or property resulting from any ideas, methods, instructions or products referred to in the content.